Isomerization of Olefin Radical Cations in ZSM-5 Zeolites†

D. W. Werst,* E. E. Tartakovsky, E. A. Piocos, and A. D. Trifunac*

Chemistry Division, Argonne National Laboratory, Argonne, Illinois 60439

Received: May 30, 1994; In Final Form: July 29, 1994⊗

Variable-temperature EPR was used to investigate reactions of olefin radical cations generated radiolytically in nonacidic and acidic ZSM-5 zeolites. The olefin radical cations undergo isomerization reactions even at 4 K. Radical cation reactions are presumably driven by the exothermicity of charge transfer, which is not efficiently quenched by the vibrational modes of the zeolite lattice. The observation of H-addition type radicals indicates Bronsted acid-catalyzed rearrangements prior to irradiation on the more acidic zeolites.

1. Introduction

Zeolites are unique microporous materials that support many approaches to nanoscale engineering through synthetic modification and introduction of adsorbed molecules.[1−6] Their pore dimensions, which are comparable to the diameters of small molecules (5-13 Å), lead to shape- and size-selective phenomena and, in some cases, highly specific chemical reactivity. The ZSM-5 family of aluminosilicates are important in many industrial processes. The acidic forms of ZSM-5 zeolites are active catalysts and are widely used in the petroleum industry for conversion of small hydrocarbons and alcohols and cracking of olefins and alkanes.[1,7]

The catalytic activity of the H^+ form of ZSM-5 is generally ascribed to reactions of substrate molecules with Bronsted acid sites (acidic hydroxyls) in the zeolite to form reactive proton adducts.[8−11] For example, protonation of alkenes on H-ZSM-5 and other acidic zeolites followed by chemical transformations of the resulting carbenium ions accounts for the product spectrum, which includes isomers and oligomers of the starting material.[10,12−19] The carbenium ion formalism is in analogy to reaction mechanisms of olefins in mineral acids and superacids, which the solid acid chemistry, to a large degree, mimics. Free carbenium ions in zeolites, however, are probably rare because interactions with adjacent oxygens on the surface confer a degree of covalent character.[8] In this paper, we will often allude to "carbenium ions" on H-ZSM-5, while acknowledging that their true nature lies somewhere intermediate between free ions and covalently bound alkoxides.

Less attention has been addressed to the catalytic activity of Lewis acid sites and spontaneous oxidation of adsorbed molecules that results in chemical transformations involving highly reactive radical cation intermediates.[20] EPR studies of paramagnetic intermediates (radical cations and neutral radicals) that are formed following activation of H-ZSM-5 and H-Mordenite and subsequent exposure to hydrocarbon molecules indicate that oxidation processes can be important.[21−28]

We have employed variable-temperature EPR to investigate *radiolytically generated* radical cations in zeolites.[29−35] Zeolites satisfy the fundamental requirements for matrix stabilization of radical cations, i.e., they possess high ionization potentials and trap electrons that would otherwise recombine with the radical cations. We have shown that γ- or electron-irradiated zeolites are capable of oxidizing a wide range of organic molecules. The steps involved in radiolytic generation of radical cations in zeolites can be depicted as in eqs 1 and 2.

$$Z \xrightarrow[e^- \text{ beam}]{\gamma \text{ or}} Z^{\bullet+} + e^-(\text{trapped}) \quad (1)$$

$$Z^{\bullet+} + M \rightarrow Z + M^{\bullet+} \quad (2)$$

Z denotes the constituent part of the zeolite framework that is ionized upon radiolysis, and M is a substrate molecule. At low temperatures, the substrate radical cations (as well as the unoxidized substrate molecules) are immobilized in the pores of the zeolite.

Zeolites have manifold other qualities that make them versatile matrices for EPR studies of radical cations. Zeolites are stable well above the decomposition temperatures of the substrate molecules, and thus variable-temperature studies are not bounded by the softening point of the matrix as in traditional matrices, such as neon (mp = 27 K), argon (mp = 87 K), or halocarbons (mp = 110−160 K). The irradiated zeolites give very little background EPR signal. Depending on the fit between the substrate and the zeolite cavity, radical cations in zeolites often retain greater motional freedom than radical cations frozen in molecular solvents, which can lead to more isotropic hyperfine and **g** tensors and better resolved EPR spectra. Finally, the zeolite−radical cation interaction can be tuned by varying the (1) charge-balancing cation (H^+, Na^+, Cu^{2+}, etc.), (2) silicon-to-aluminum ratio (relative acidity), and (3) pore size, etc. In summation, the zeolite matrix represents a unique test reactor for radical cation intermediates that allows a significant measure of experimental control over molecular orientation and ion−molecule encounters. The zeolite−radical cation interactions can even influence reaction potentials and the relative energies of radical cation electronic states.[30,32,33]

In addition to investigating radical cation structure and reactivity in zeolites, our work sheds light on the possible role of radical cations in zeolite catalysis. Simple EPR studies of spontaneous oxidation in acidic zeolites are clouded by the possible occurrence of carbocation chemistry. In many cases, isomeric or dimer radical cations are observed.[21,23,24] Previous studies have not been able to determine whether the observed radical cations are formed via reaction of oxidized substrate molecules or oxidation of the products of carbenium ion reactions. Resolving the roles of Bronsted acid activity and Lewis acid activity requires a multidimensional approach. Our approach allows us to generate radical cations in any zeolite, including nonacidic zeolites, and thus characterize the intrinsic radical cation reactivity in zeolites in the absence of Bronsted acid catalysis. Results in nonacidic zeolites can in turn be

† Work performed under the auspices of the Office of Basic Energy Sciences, Division of Chemical Science, US-DOE, under contract number W-31-109-ENG-38.

⊗ Abstract published in *Advance ACS Abstracts,* September 1, 1994.

0022-3654/94/2098-10249$04.50/0

compared to the fate of radical cations generated radiolytically in acidic zeolites and by spontaneous oxidation processes.

In this work, we observed bond and skeletal rearrangements of radical cations of 1,4-cyclohexadiene, 2,3-dimethyl-1-butene, and 3,3-dimethyl-1-butene on acidic and nonacidic ZSM-5 zeolites. As in past examples from our laboratory, we found the radical cations to be more reactive in zeolites than in frozen molecular solvents such as freons. We attribute the observed isomerizations in zeolites to reactions of nonthermalized radical cations and suggest that the zeolite lattice is a poor heat sink for excess vibronic energy in the radical cations. Methyl-substituted butenes have been used in tests of acid catalysis in zeolites and thus provide a good link to the catalysis studies. Some involvement of Bronsted acid-catalyzed reactions prior to radiolysis is indicated by the observation of H-addition type radicals.

2. Experimental Section

The Na-ZSM-5 and H-ZSM-5 zeolites were kindly donated by Chemie Uetikon (Switzerland). The SiO_2/Al_2O_3 ratios were 170 for the Na-ZSM-5 and 240 for the H-ZSM-5. The almost aluminum-free form of ZSM-5, silicalite, was a gift from Union Carbide (silicalite-S115). All alkenes and freons were used as received from Aldrich. 2,3-Dimethylbutane was obtained from Phillips and purified by passing through activated silica gel.

Silica sol-gels were made by hydrolysis of tetramethoxysilane (Aldrich or Fluka) in methanol at neutral pH. The amount of water used was in a mole ratio of 2.5:1 water:tetramethoxysilane. The solutions were stirred for 0.5 h at room temperature, sealed tightly in polypropylene bottles, and transferred to a 60 °C oven where they gelled within 2 h. The gels were aged for 24 h at 60 °C. After aging, the gels were dried at 60 °C. The dried sol-gel was pulverized and treated in the same manner as described below for zeolite samples.

Zeolite samples were prepared on a glass vacuum manifold in 4 mm diameter Suprasil EPR tubes. The EPR tube containig 50 mg of the zeolite powder was evacuated ($\leq 10^{-4}$ Torr) and then heated to at least 673 K for 4−6 h or more. A measured amount (0.1−6% by weight) of the chemical of interest, after several freeze−pump−thaw cycles, was adsorbed from the vapor phase onto the activated zeolite at room temperature. If adsorption was slow, liquid nitrogen was used to cool the sample tube and condense the desired amount of vapor. The sample tube was sealed under vacuum while the loaded zeolite powder was held at liquid nitrogen temperature. The sealed sample was equilibrated at room temperature overnight or longer prior to irradiation.

No EPR signals were observed in any sample after equilibration and prior to irradiation. No EPR signals were observed in two H-ZSM-5 samples that were tested immediately after loading 2% 1,3-cyclohexadiene and 1,4-cyclohexadiene, respectively.

The majority of zeolite samples were irradiated by a ^{60}Co γ source at 77 K to a dose of approximatley 0.3 Mrad and subsequently transferred to the liquid helium cryostat in the EPR spectrometer. Alternatively, samples were irradiated by 3 MeV electrons from a Van de Graaff electron accelerator *in situ* in the liquid helium cryostat of the EPR spectrometer. This capability allowed the irradiation and the EPR observation at temperatures down to 4 K. The dose delivered with the electron beam was comparable to that from the γ source.

After irradiation, EPR spectra were collected between 4 K and room temperature at appropriate intervals; spectral cahnges were tested for reversibility. Two EPR spectrometers were used, a Varian E-109 EPR spectrometer and a Bruker series ER 200 EPR spectrometer. Both spectrometers were equipped with a Heli-Tran liquid helium transfer cryostat (APD) for temperature control from 4 K to room temperature. Magnetic field control and data acquisition were accomplished with a LabVIEW program (National Instruments) on a Macintosh II computer.

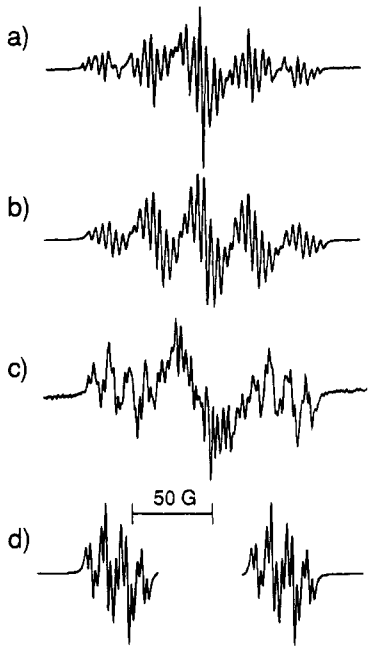

Figure 1. EPR spectra observed at (a) 100 and (c) 160 K after 77 K γ irradiation of 2% 1,4-CHD in Na-ZSM-5. The calculated spectrum of 1,3-CHD$^{\bullet+}$ is shown in b with the coupling constants taken from the literature (Table 2). The spectrum of the cyclohexadienyl radical (d) was calculated with the coupling constants 51 (2H), 13 (H), 9.3 (2H), and 2.7 G (2H) to fit the experimental spectrum (c). These values are very close to those in the literature. The central portion of the cyclohexadienyl spectrum, complicated by second-order hyperfine structure, is omitted from the calculated spectrum.

TABLE 1: Gas-Phase Heats of Formation, ΔH_f (kcal/mol), of Radical Cations and Ionization Potentials, IP (eV), of the Neutral Precursors (ref 36)

radical cation	abbreviation	ΔH_f	IP
1,4-cyclohexadiene$^{\bullet+}$	1,4-CHD$^{\bullet+}$	229	8.8
1,3-cyclohexadiene$^{\bullet+}$	1,3-CHD$^{\bullet+}$	216	8.25
3,3-dimethyl-1-butene$^{\bullet+}$	3,3-DMB-1$^{\bullet+}$	203	9.5
2,3-dimethyl-1-butene$^{\bullet+}$	2,3-DMB-1$^{\bullet+}$	194	9.1
tetramethylethylene$^{\bullet+}$	TME$^{\bullet+}$	174	8.3

3. Results

All of the olefin radical cations studied rearranged during irradiation to a more stable radical cation. The transformations involved double-bond migration and skeletal rearrangement. The parent radical cation was generally not observed, even when the irradiation was carried out at 4 K. The first example is the isomerization of 1,4-cyclohexadiene radical cation (1,4-CHD$^{\bullet+}$) to give the 1,3-cyclohexadiene radical cation (1,3-CHD$^{\bullet+}$). Figure 1a shows the EPR spectrum observed in Na-ZSM-5 containing 2% 1,4-CHD, recorded at 100 K after γ irradiation at 77 K. The spectrum reveals 100% conversion to 1,3-CHD$^{\bullet+}$. (The identical spectrum was observed in a zeolite sample loaded with 2% 1,3-CHD). Similar results were obtained in silicalite and silica sol-gels prepared by us.

The isomerization of 1,4-CHD$^{\bullet+}$ to 1,3-CHD$^{\bullet+}$ is an energy-downhill process with a gas-phase exothermicity of 13.4 kcal/mol (Table 1). This reaction was observed by Shida et al. in a freon matrix but only upon photoexcitation with near infrared light (λ > 700 nm).[37] 1,4-CHD$^{\bullet+}$ was also shown to be stable

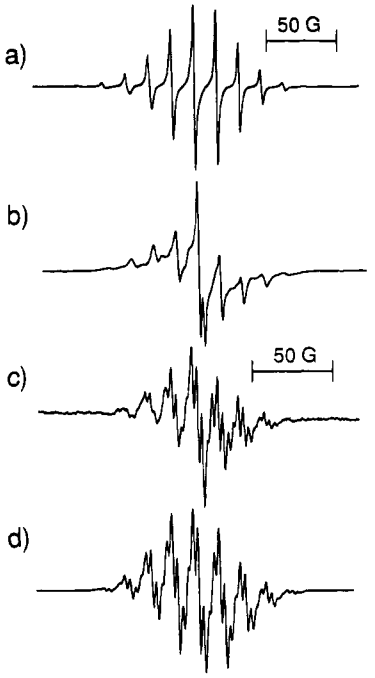

Figure 2. EPR spectra observed at (a) 77 and (c) 230 K after 77 K γ irradiation of 2% 2,3-DMB in silicalite and at (b) 77 K in slilica sol-gel loaded with 2% 2,3-DMB. The calculated spectrum (d) of the 1,1,2-trimethylallyl radical is shown with the coupling constants taken from the literature (Table 2).

on the submicrosecond time scale in cooled methylcyclohexane liquid.[38] In the zeolite, the 1,3-CHD$^{\bullet+}$ spectrum is exclusively generated down to 4 K, albeit less resolved at low temperature because of slower ring inversion. The wide quintet EPR spectrum (a = 68 G) of planar 1,4-CHD$^{\bullet+}$ exhibits no significant temperature dependence and is readily distinguished from the EPR spectrum of 1,3-CHD$^{\bullet+}$.[37]

Transformation of radical cations to neutral radicals via ion–molecule reactions is commonly observed in the condensed phase, and zeolites are no exception.[31-33] 1,3-CHD$^{\bullet+}$ is converted to the cyclohexadienyl radical in zeolites upon annealing (Figure 1c). The result was invariant for 1,4-CHD or 1,3-CHD as substrate. The onset temperature for this process was approximately 120 K. The conversion was complete as shown by the excellent agreement between the experimental and calculated EPR spectra for the cyclohexadienyl radical.[39] The central portion of the cyclohexadienyl radical spectrum is highly congested due to second-order hyperfine structure. The spectrum consists of four equivalent sets of lines, the inner two sets overlapping.[39] The outer two sets agree very well with the calculated spectrum. As our simulation program does not calculate hyperfine couplings to second order, no attempt was made to simulate the central portion of the spectrum.

Figures 2 and 3 illustrate transformations of both 2,3-dimethyl-1-butene radical cation (2,3-DMB-1$^{\bullet+}$) and 3,3-dimethyl-1-butene radical cation (3,3-DMB-1$^{\bullet+}$) to give the tetramethylethylene radical cation (TME$^{\bullet+}$) on nonacidic zeolites and silica sol-gels. These reactions have gas-phase exothermicities of 20 and 29 kcal/mol for 2,3-DMB-1$^{\bullet+}$ and 3,3-DMB-1$^{\bullet+}$, respectively (Table 1). The EPR spectrum observed at 77 K after irradiation of silicalite containing 2% 2,3-DMB-1 is shown in Figure 2a. Eleven lines of the 13-line multiplet (a = 17.1 G) due to coupling to 12 equivalent hydrogens were observed. The symmetric TME$^{\bullet+}$ is an EPR spectroscopist's delight because of the single hyperfine coupling constant and the lines made narrow by free methyl rotation and small hyperfine anisotropy associated with β-hydrogens of olefin

TABLE 2: Literature Values of Proton Hyperfine Coupling Constants, a (G), for Radical Cations and Radicals in This Study (1 G = 0.1 mT)

	solvent	T (K)	a		ref
		Radical Cation			
1,4-CHD$^{\bullet+}$	$CFCl_3$		68.0	$-CH_2-$	37
1,3-CHD$^{\bullet+}$	$CFCl_3$	130	42.4	$2H_\beta$ (axial)	37
			13.4	$2H_\beta$ (equatorial)	
			8.4	$-CH=$ (terminal)	
			4.2	$-CH=$ (inner)	
TME$^{\bullet+}$	MCH[a]	190	17.1		43
	$CFCl_3$	77	17.2		37
		Radical			
cyclohexadienyl	1,4-CHD	290	47.70	$-CH_2-$	39
			8.99	ortho $-CH=$	
			2.65	meta $-CH=$	
			13.04	para $-CH=$	
cyclohexenyl	adamantane	216	14.63	2H (1,3)	44
			3.57	H (2)	
			26.49	2H (4,6)	
			8.44	2H (4′,6′)	
			0.89	2H (5,5′)	
1,1,2-trimethylallyl	$CF_2ClCFCl_2$	125	16.0	$3H_{exo}$	42
			12.7	$3H_{endo}$	
			13.5	2H	
			3.3	3H	
tetramethylethyl	cyclopropane	150	22.92	6H	45
			9.8	H	

[a] MCH = methylcyclohexane.

radical cations. This multiplet structure with characteristic sharp lines makes the assignment of TME$^{\bullet+}$ unmistakable. The parent radical cation, 2,3-DMB-1$^{\bullet+}$, was not observed, even at 4 K. Similar results were obtained in Na-ZSM-5 and sol-gels. The quality of the EPR spectra in the sol-gel was lower (Figure 2b), in part due to greater background signal from the irradiated sol-gel matrix, but the TME$^{\bullet+}$ EPR spectrum is clearly discernible.

The EPR spectra generated in mixtures of 2,3-DMB-1 and different freons ($CFCl_3$ and $CF_2ClCFCl_2$) were extremely matrix dependent, as is the case for radical cations of other simple olefins such as propylene and methyl-substituted propylenes.[40] In contrast to the neutral parent molecules, radical cations of simple olefins (apart from TME$^{\bullet+}$) are found to deviate from planarity at the C–C double bond. The twist angle, and thus the hyperfine coupling constants (in particular, hyperfine coupling constants for the α-hydrogens), is quite sensitive to the physical environment. We therefore are left with no reliable reference for the 2,3-DMB-1$^{\bullet+}$ EPR spectrum for comparison to the present work in zeolites. Nonetheless, we can confidently conclude that it contributes negligible signal intensity in Figure 2a.

Annealing the silicalite sample converted TME$^{\bullet+}$ to the 1,1,2-trimethylallyl radical, $C_6H_{11}^{\bullet}$ (Figure 2c). The TME$^{\bullet+}$ signal disappeared completely, leaving only the spectrum of the trimethylallyl radical. The temperature for onset of this process was approximately 160 K. The same reaction was previously observed for TME loaded on silicalite, on Na-X,[41] and in $CF_2ClCFCl_2$.[42] In zeolite Na-X, $C_6H_{11}^{\bullet}$ was the only radical species observed after irradiation at 77 K; TME$^{\bullet+}$ was not stabilized. In the freon, annealing first gives rise to the dimer radical cation, $(TME)_2^{\bullet+}$ (a(24H) = 7.8 G), which decays and is replaced by the trimethylallyl radical upon further temperature increase. No dimer radical cation intermediate was observed in the present study.

The annealing behavior of 2,3-DMB-1 samples in Na-ZSM-5 deviated from the pattern of proton loss from the radical cation, i.e., TME$^{\bullet+}$. While the low-temperature behavior was the same as in silicalite, the TME$^{\bullet+}$ signal persisted up to room temperature where it decayed with a time constant of minutes. The 1,1,2-trimethylallyl radical was not observed. A small yield

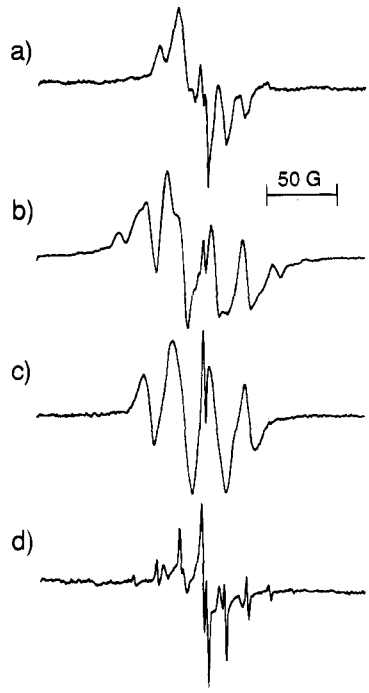

Figure 3. EPR spectra observed at (a) 77 and (d) 185 K after 77 K γ irradiation of 5.7% 3,3-DMB in silicalite. The EPR spectra observed at (b) 77 and (c) 105 K are shown for an irradiated 1:1000 mixture of 3,3-DMB and $CF_2ClCFCl_2$. The sharp central spike that is most pronounced in c is the characteristic background signal from the irradiated Suprasil sample tube.

of a different radical species was observed, but the ratio of this weak signal to that of $TME^{\bullet+}$ was not significantly temperature dependent (*vide infra*).

The $TME^{\bullet+}$ spectrum was observed immediately after irradiation in *some* samples of 3,3-DMB-1 in nonacidic zeolites; in other samples, a different precursor species was observed prior to the growth of the $TME^{\bullet+}$ signal. $TME^{\bullet+}$ always appeared upon annealing (Figure 3d). The temperature of onset of clear $TME^{\bullet+}$ lines was variable. The EPR spectrum observed at 77 K after irradiation of silicalite containing 5.7% 3,3-DMB-1 is shown in Figure 3a. (Similar results were obtained for 2% 3,3-DMB-1.) It is assumed that this signal is due to a radical cation since it appears to be the precursor of $TME^{\bullet+}$. The changeable EPR results for different 3,3-DMB-1 samples may be related to sample preparation (zeolite activation conditions, temperature during adsorption, equilibration time, oxygen contamination, etc.), although care was taken to reproduce these as closely as possible.

Our attempts to generate the EPR spectrum of the parent radical cation, 3,3-DMB-$1^{\bullet+}$, in freon matrices was again complicated by the extreme matrix dependence of the resulting spectra, no doubt for the same reason stated earlier, i.e., the matrix dependence of the twist angle and thus the hyperfine coupling constants. The nearest resemblance to the spectrum in Figure 3a was obtained in a 1:1000 mixture of 3,3-DMB-1 and $CF_2ClCFCl_2$. At 105 K (Figure 3c), a quartet with approximately 26 G spacing is observed, consistent with coupling to three nearly equivalent hydrogens, presumably the three α-hydrogens of 3,3-DMB-$1^{\bullet+}$. At 77 K (Figure 3b), additional hyperfine structure is observed. While 3,3-DMB-$1^{\bullet+}$ is a likely assignment for the precursor species in Figure 3a, we cannot rule out other possible $C_6H_{12}^{\bullet+}$ intermediates, including 2,3-DMB-$1^{\bullet+}$.

Isomerized radical cations were also observed on H-ZSM-5 loaded with 1,4-CHD, 2,3-DMB-1, and 3,3-DMB-1. Figures 4 and 5 illustrate the EPR results following irradiation of 3,3-DMB-1 on H-ZSM-5. Irradiation at 77 or 4 K of H-ZSM-5 containing 3,3-DMB-1 always gave rise immediately to the signal from $TME^{\bullet+}$. Again, the EPR results showed some sample variation. The data can be divided into two sets; in some samples, $TME^{\bullet+}$ was the only radical cation species observed following irradiation, and in other samples, the EPR spectra showed a significant admixture of one additional species.

Figure 4 shows the very low-temperature behavior of a 3,3-DMB-1 sample on H-ZSM-5. After irradiation at 77 K, the only species observed was $TME^{\bullet+}$. Upon lowering the sample temperature to 4 K, a doubling of lines was observed (in some, not all, samples) as shown in Figure 4a. This is shown here because it represents the only observation in our study that was reminiscent of EPR signals due to $(TME)_2^{\bullet+}$, which should give one-half the coupling constant of $TME^{\bullet+}$ and 25 lines instead of 13.[42,43] However, the formation of $(TME)_2^{\bullet+}$ would be surprising indeed under the assumption that the neutral substrate molecules in the proximity of the radical cations are all 3,3-DMB-1. Besides, no mobility of neutral or ionic species is possible below 77 K in the zeolite, and therefore dimer-forming encounters are not likely. The lines at half-spacing decrease in intensity with modest warming and vanish above 30 K (Figure 4a–d). Dissociation of a preformed dimer at such low temperatures is in contrast with EPR results showing that $(TME)_2^{\bullet+}$ is stable at 110 K in $CF_2ClCFCl_2$.[42]

A more plausible explanation for the observed doubling of lines and half-spacing is E lines produced by the quantum mechanical tunneling rotation of methyl groups.[46–52] E lines have been observed in this same temperature range for many other radicals containing methyl groups.[46–51] When the temperature for the 3,3-DMB-1 sample was restored to 4 K, the spectrum in Figure 4e was observed in which the E lines have regained only part of their original intensity. Howerver, 15 min later, the spectrum in Figure 4f was observed, indicating a lag time in the tempertaure equilibration of the sample. This behavior exaclty parallels that in EPR studies of *tert*-butyl radicals near 4 K.[48]

In other 3,3-DMB-1 samples (and one 2% 2,3-DMB sample) on H-ZSM-5, a broad signal was superimposed on the sharp $TME^{\bullet+}$ EPR spectrum. The relative amount of the broad signal varied from sample to sample and did not necessarily scale with substrate concentration. The spectrum observed in one such sample is shown in Figure 5a. We estimate that >80% of the total signal intensity is due to the broad component. The assignment of the broad component is uncertain, and it does not match the signal observed in nonacidic zeolites containing 3,3-DMB-1 (Figure 3a). On the other hand, very close resemblance was found to the spectrum observed in Na-ZSM-5 containing another C_6H_{12} isomer, 2-methyl-2-pentene (Figure 5b). The energy of the 2-methyl-2-pentene radical cation is intermediate between 2,3-DMB-$1^{\bullet+}$ and $TME^{\bullet+}$.[36] We observed no strong evidence that the broad component is converted to $TME^{\bullet+}$ upon annealing. The spectrum shown in Figure 5b was also observed in H-ZSM-5 loaded with 2-methyl-2-pentene, but it was superimposed on the spectrum of $TME^{\bullet+}$.

In acidic zeolites containing any of the C_6H_{12} isomers (TME, 2,3-DMB-1, 3,3-DMB-1), the $C_6H_{11}^{\bullet}$ radical was not formed upon annealing and the $TME^{\bullet+}$ signal was very persistent. It survived to room temperature, although with noticeable intensity loss in a period of minutes to hours. Alongside the $TME^{\bullet+}$ signal, however, we observed a weak signal due to the tetramethylethyl radical, $(CH_3)_2CHC^{\bullet}(CH_3)_2$. The tetramethylethyl radical, $C_6H_{13}^{\bullet}$, has an EPR spectrum in the zeolite consisting of a septet of doublets, $a(6H) = 23.4$ G and $a(H) = 5.5$ G (Figure 6a). While the septet coupling constant is very

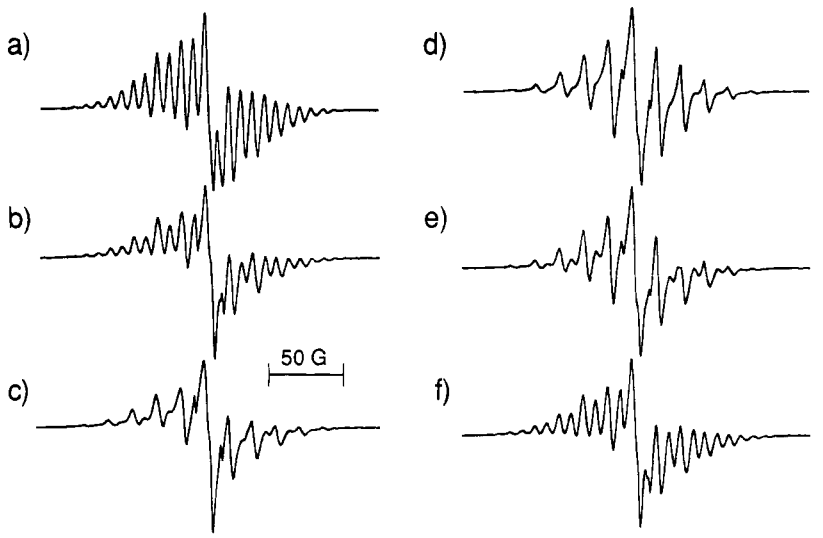

Figure 4. Temperature dependence of the intensity of E lines in γ-irradiated H-ZSM-5 containing 2% 3,3-DMB: (a) 4, (b) 12, (c) 18, and (d) 27 K. The samples was stored at 77 K overnight and the experiment repeated the next day: (e) 4 K, (f) same as e, 15 min later.

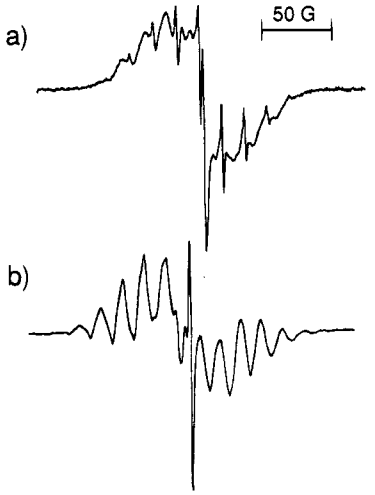

Figure 5. EPR spectra observed at 77 K after 77 K γ irradiation of (a) 0.5% 3,3-DMB in H-ZSM-5 and (b) 2% 2-methyl-2-pentene in Na-ZSM-5. The sharp central spike is the characteristic background signal from the irradiated Suprasil sample tube.

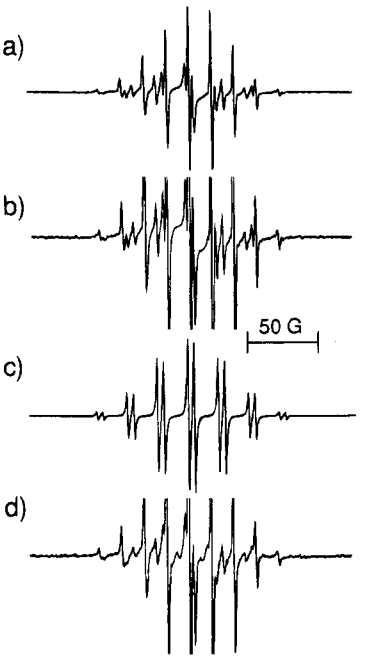

Figure 6. EPR spectra observed after 77 K γ irradiation of (a) 2% 3,3-DMB in H-ZSM-5, T = 205 K; (b) 2% TME in H-ZSM-5, T = 205 K; and (d) 2% 2,3-DMB in Na-ZSM-5, T = 245 K. The spectrum of the tetramethylethyl radical was simulated (c) with the coupling constants 23.4 (6H) and 5.5 G (H), which fit the experimental spectrum.

near the value obtained in the liquid phase, the coupling constant for the lone hydrogen is roughly 40% lower than in the liquid.[45] This is understandable, since the coupling to the lone hydrogen in tetrasubstituted ethyl radicals is highly dependent on the conformation and can even become vanishingly small as the radical geometry relaxes to minimize steric interactions.[45] While the α-methyl groups are freely rotating, the conformation about the central C—C bond is locked and should be matrix dependent.

Figure 6b shows an expanded view of the C_6H_{13}• signal in a sample of H-ZSM-5 containing 2% TME. Assignment of this radical in the H-ZSM-5 samples allowed us to recognize that the same radical, in smaller yield, is formed in Na-ZSM-5 with 2,3-DMB-1 (Figure 6d). The temperature of onset of the C_6H_{13}• was difficult to determine because its EPR spectrum begins to broaden below 100 K (*vide infra*). We could not rule out the possibility that it is formed during irradiation.

An alternate pathway to $TME^{\bullet+}$ in zeolites was found to be H_2 elimination from the 2,3-dimethylbutane radical cation. This reaction was studied previously in low-temperature hydrocarbon matrices[53] and *n*-pentane solutions.[54] Figure 7a shows the EPR spectrum observed in silicalite containing 3.3% 2,3-dimethylbutane. The EPR spectrum of the parent radical cation is most recognizable at low temperature where the conformations of the methyl groups are locked, and the spectrum is a quintet due to coupling to one hydrogen per methyl group. The spectrum observed in the zeolite at 4 K (after irradiation at 77 K) shows that the dominant signal is due to the radical cation of 2,3-dimethylbutane. The stick spectrum was simulated with a 37 G spacing.[55]

Above 77 K, the spectrum begins to break up into a mixture of signals from $TME^{\bullet+}$ and the tetramethylethyl radical. In fact, the $TME^{\bullet+}$ lines are discernable already at 77 K. It is impossible to judge whether a small amount of $TME^{\bullet+}$ formed during irradiation is obscured at low temperature by the broad spectrum of the 2,3-dimethylbutane radical cation or some conversion occurs during storage at 77 K as in the hydrocarbon.[53]

The C_6H_{13}• signal becomes dominant upon annealing the 2,3-dimethylbutane samples (Figure 7b). When the temperature is returned to 77 K (Figure 7c), the C_6H_{13}• spectrum broadens appreciably and the 5.5 G doublet splitting is not resolved. This

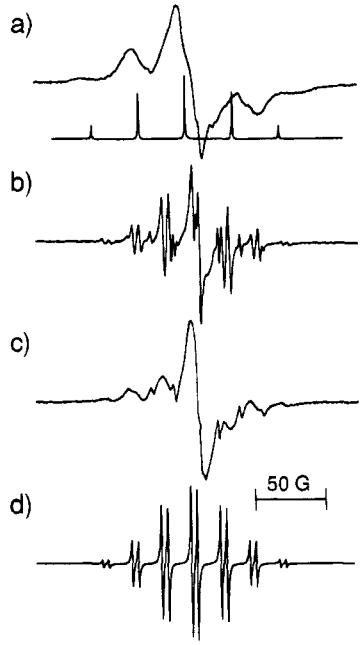

Figure 7. EPR spectra observed at (a) 4 and (b) 175 K after 77 K γ irradiation of 3.3% 2,3-dimethylbutane in silicalite. Reversible line broadening causes the doublet hyperfine structure in the tetramethylethyl EPR spectrum to be unresolved when the sample temperature is returned to 77 K (c). The calculated spectrum of the tetramethylethyl radical, 23.4 (6H) and 5.5 G (H), is reproduced in d.

temperature-dependent line broadening makes it impossible to detect the tetramethylethyl radical EPR signal at 77 K in the presence of a dominant signal from $TME^{\bullet+}$ (i.e., in the butene samples). The sharp interior lines due to $C_6H_{13}^{\bullet}$ (e.g., Figure 6a,b) appear to recede into the base line when the sample temperature is returned to 77 K.

The discovery of $C_6H_{13}^{\bullet}$ radicals in acidic zeolites containing the C_6H_{12} olefins led us to reinvestigate both cyclohexadiene isomers in H-ZSM-5. The dominant process upon annealing was decay of the 1,3-$CHD^{\bullet+}$ signal and appearance of the cyclohexadienyl radical, $C_6H_7^{\bullet}$, just as observed in nonacidic zeolites. However, upon decay of the cyclohexadienyl radical at 170−190 K, a small residual EPR signal due to the cyclohexenyl radical, $C_6H_9^{\bullet}$, was observed. Assignment of the cyclohexenyl spectrum was confirmed by comparing it to the cyclohexenyl radical spectrum observed in cyclohexene-loaded Na-ZSM-5 upon decay of the cyclohexene radical cation. The cyclohexenyl radical spectrum in zeolites closely resembles that observed in solution.[44]

4. Discussion

4.1. Radical Cation Isomerization. We have illustrated several isomerization reactions of olefin radical cations on zeolites, eqs 3−5, that are analogous to transformations of butenes and methyl-substituted butenes catalyzed by acidic zeolites.[12−19] The bulk of radical cation reactions in our study

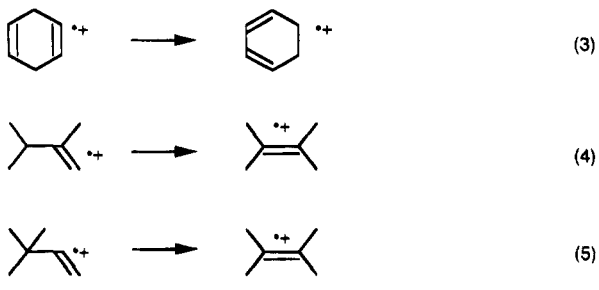

were carried out on highly siliceous forms and Na forms of ZSM-5 zeolites so as to minimize Bronsted acid sites and the possible involvement of carbenium ion chemistry. Silica sol-gels, which are entirely aluminum-free but otherwise not well characterized with respect to acidic hydroxyl content, were also used. The conversion of the parent radical cations to the more stable isomers in most cases was complete. One hundred percent reaction is strong evidence that our observations are not due to small residual amounts of acidic sites in these matrices.

The unique aspect of the radical cation isomerization reactions in zeolits is that they occur even at 4 K. Such rearrangements also occur in halocarbon matrices, but only following photo-excitation; the parent radical cations are in general stable at thermal energies.[37,56] What are the energy requirements for radical cation isomerization in zeolites, and what is the source of energy for promoting the observed reactions?

The energy barriers to olefin radical cation isomerization can be rather small (1-2 eV). The reaction of 1,4-$CHD^{\bullet+}$ to give 1,3-$CHD^{\bullet+}$ is driven in freon matrices by light with wavelength > 700 nm.[37] The charge−resonance transition responsible for the 1,4-$CHD^{\bullet+}$ absorption in the near IR is approximately 1 eV.[37] Similarly, the isomerization of the 1-butene radical cation to the 2-butene radical cation is also promoted in freon matrices by light λ > 700 nm (< 1.7 eV).[56]

Our previous work has shown that radical cation−zeolite interactions can modify reaction potentials and lower barriers to thermal reactions of radical cations.[32,33] Thermally activated isomerization and bond-scission reactions have been observed at lower temperatures in zeolites than in other matrices. Therefore the energy requirements for the olefin radical cation isomerizations in zeolites may be lower than the above estimates; however, the reaction of *thermalized* radical cations at 4 K implies that the reaction barrier is vanishingly small.

On the other hand, the occurrence of the radical cation reactions during irradiation means that we cannot exclude reactions of *nonthermalized* radical cations. Electron transfer from sorbate molecules to the ionized matrix is exothermic and can appear as vibrational and/or electronic excitation in the newly formed radical cation. The ability of the matrix to stabilize a metastable radical cation that is capable of rearranging to a lower energy isomer depends on its efficiency as a heat sink. While freon matrices are in general very efficient at removing excess energy from primary radical cations and preventing reactions, the absence of suitable vibrational modes and poor energy coupling between substrate ion and matrix is one of the principal drawbacks of rare gases when used for matrix-isolation studies.[57] Zeolites may be expected to be intermediate between these two cases.

The charge-transfer exothermicity can best be estimated from the difference in gas-phase ionization potentials of the matrix and the substrate molecules. Gas-phase ionization potentials of fluorochlorocarbons used for EPR studies of radical cations fall in the range 11.5−12 eV,[36] compared to 15.7 and 12.1 eV for argon and xenon, respectively. The effective ionization potential for zeolites can be estimated from the ability of the radiolyzed zeolite to ionize substrate molecules of increasing ionization potential. The ionization of alkanes in irradiated zeolites places a lower limit for the zeolite effective potential between 10 and 10.5 eV. Recent studies of acetylene in zeolites in our laboratory suggest that the irradiated zeolite is capable of ionizing substrate molecules with an ionization potential of 11.5 eV or greater.[58]

The olefins in the present study possess gas-phase ionization potentials less than 9.5 eV (Table 1). Therefore, 1−2 eV or

more excess energy is available to the nascent radical cations. The most plausible explanation for the inability of the zeolite to stabilize the parent olefin radical cations is that the excess energy is used to drive the chemical reaction before it is dissipated as heat to lattice vibrations.

It is not yet safe to generalize that chemical reactions of radical cations compete efficiently with deactivation in zeolites, that is, that zeolites are inherently weak at stabilizing all metastable radical cations. The 2,3-dimethylbutane radical cation, which undergoes H_2 elimination at small thermal energies in hydrocarbon solvents,[53] can be stabilized and observed in zeolites. Evidence reported by us of the detection of the quadricyclane radical cation suggests that this very elusive radical cation, which easily isomerizes to the norbornadiene radical cation, is stabilized in zeolites at very low temperatures (<30K).[34] Clearly, more examples are needed to establish trends of radical cation reactivity in zeolites. As in so many behaviors associated with zeolites, one might expect radical cation reactions in zeolites to exhibit great selectivity and depend critically on the details of the radical cation−zeolite interactions.

4.2. Radical Formation. At least two mechanisms of neutral radical formation can be inferred from our results. An H-loss mechanism results in the radicals cyclohexadienyl and 1,1,2-trimethylallyl. These radicals are derived from the radical cation precursor; decay of the radical cation signal is accompanied by the growth of the neutral radical signal upon annealing. This reaction causes the complete conversion of the radical cation to the neutral radical. An H-addition mechanism results in the cyclohexenyl and tetramethylethyl radicals. These radicals coexist with the radical cations and are probably not derived from radical cation precursors. They are formed in small yield, during irradiation.

The familiar mechanism is formal hydrogen loss that occurs in two steps: (i) one-electron oxidation (ionization) and (ii) radical cation deprotonation. In the present work, step i is accompanied by isomerization. Proton loss is a primary mechanism of radical cation decay in the condensed phase and usually occurs via ion−molecule reactions between radical cations and their neutral parent molecules. Ion−molecule reactions of radical cations have been studied by time-resolved methods in solution[59−61] as well as by matrix-isolation in freons[42,62,63] and zeolites.[31−33,35]

In solid matrices, the telltale pattern for ion−molecule reactions is the gradual replacement of the radical cation signal by that of the neutral radical as the temperature is increased and diffusional encounters occur between ions and neutrals. In freon matrices, the onset temperature for such reactions correlates with the softening point of the matrix or known phase transition. Diffusional behavior in zeolites is more complicated, and the onset temperature is harder to predict. The onset temperature for different ion−molecule reactions varies greatly and sometimes decreases with increasing substrate concentration. Assuming that radical cations are less mobile than neutral molecules because of electrostatic interactions with the zeolite, ion−molecule encounters are brought about principally by diffusion of neutral substrate molecules to the ions.

The behavior of certain radical cations we have studied is not consistent with a mechanism of thermally activated diffusion and ion−molecule reaction. Anomalies include the appearance of neutral radicals at low temperatures where diffusion is not possible and an inverse concentration dependence where the radical to radical cation ratio increases with decreasing substrate loading. This has led us to consider an alternative mechanism for radical cation deprotonation in zeolites, which is proton transfer to basic sites in the matrix (i.e., lone pairs on oxygen atoms). This issue is beyond the scope of the present paper; a full study will be presented in a future publication.[64] The behavior observed for the formation of cyclohexadienyl and trimethylallyl radicals in this study is consistent with the "normal" mode of radical cation decay in the solid state, that is, ion−molecule reaction.

An unresolved question related to the ion−molecule decay of radical cations is whether the mechanism is proton transfer from the radical cation to the neutral molecule or hydrogen atom transfer from the neutral molecule to the ion. This assignment is ambiguous in a symmetric reaction between a radical cation and its neutral parent, the case obtained in most experiments, because the same neutral radical is produced by both mechanisms. Isomerization of the parent radical cation, however, permits us to probe the radical product of the asymmetric reaction between the isomeric radical cation and the neutral substrate. One pair of reactants in this study, $TME^{\bullet+}$ + 3,3-DMB-1, must produce distinct radical products from proton transfer and hydrogen atom transfer ($TME^{\bullet+}$ + 2,3-DMB-1 and $1,3\text{-CHD}^{\bullet+}$ + 1,4-CHD do not).

In this instance, we find support for the proton-transfer mechanism because we observe the 1,1,2-trimethylallyl radical upon decay of the $TME^{\bullet+}$ signal in silicalite when the sorbed species is 3,3-DMB-1. Formation of the trimethylallyl radical required a higher annealing temperature, and the $TME^{\bullet+}$ signal was more persistent in 3,3-DMB-1-loaded samples than in those with TME or 2,3-DMB-1. This probably reflects the influence of the bulky *tert*-butyl group on the diffusivity of 3,3-DMB-1 compared to the other two C_6H_{12} isomers.

A radical cation mechanism for the formation of the H-addition type radicals can be ruled out, as it would require the implausible hydride addition to the radical cation. We consider the inverse of the H-loss mechanism described above, i.e., protonation of neutral substrate molecules followed by one-electron reduction. In other words, carbenium ions, formed by protonation of substrate molecules at Bronsted acid sites upon adsorption at room temperature, act as scavengers of free electrons generated during radiolysis.[65] Isomerization (at room temperature) of the carbenium ion accounts for the formation of the tetramethylethyl and cyclohexenyl radicals from 3,3-DMB-1 and 1,4-CHD, respectively. The greater yield of the H-addition type radicals in more acidic zeolites is consistent with the expectation that Bronsted acid sites are necessary to form carbenium ions.

Alternatively, one might consider a mechanism involving the addition of hydrogen atoms liberated during radiolysis to the olefin substrate molecules. Hydrogen atoms are formed during radiolysis of similar materials, including types of silica glass like the Suprasil used to make our sample cells.[68] Hydrogen atoms are generated by the scission of O—H bonds in the lattice. Hydrogen atoms are stable in fused silica below 100 K,[69,70] which complicates the interrogation of H-atom signals from the zeolites. The interference of H-atom signals in the sample cells can be circumvented by time-resolved EPR techniques.[71] These experiments will be carried out in the future.

Assuming H addition to 3,3-DMB-1 gave the secondary radical, $(CH_3)_3CC^{\bullet}HCH_3$, a vicinal shift of a methyl group would be required to give the observed tetramethylethyl radical. Vicinal shifts of alkyl groups in radicals are not known[66] and are all the more unlikely at 77 K where radiolysis is carried out. Similarly, 1,2 shifts of hydrogen atoms in alkyl radicals, necessary to form the cyclohexenyl radical by H addition to 1,4-CHD, have not been demonstrated.[67]

We conclude that simple H addition to neutral substrate molecules cannot account for the formation of the H-addition

radicals. Rather, the isomerizations reflected in the formation of the tetramethylethyl and cyclohexenyl radicals are strong evidence of Bronsted acid-catalyzed reactions which occur in the zeolite samples at room temperature prior to radiolysis at 77 K. Upon γ or electron irradiation, the radicals are formed either by electron reaction with the proton adduct or by H-atom addition to isomerized substrate molecules.

4.3. Radical Cations versus Carbenium Ions. As this study points out, radical cation isomerizations on zeolites can mimic those of carbenium ions. When that is the case, it is impossible to quantitatively assess the role of Bronsted acid-catalyzed reactions, i.e., isomerization prior to radiolysis. Isomerizations on acidic zeolites of butenes and methyl-substituted butenes, through presumed carbenium ion intermediates, have been documented.[12-19] However, conversion is not complete, especially at ambient temperature.[12] Carbenium ions could give rise to the observed radical cations by the reaction sequence given in eqs 6-9 (illustrated for 3,3-DMB-1). The

$$(CH_3)_3CCH{=}CH_2 \xrightarrow{H^+} (CH_3)_3CCHCH_3^+ \quad (6)$$

$$(CH_3)_3CCHCH_3^+ \xrightarrow{\text{rearrange}} (CH_3)_2CHC(CH_3)_2^+ \quad (7)$$

$$(CH_3)_2CHC(CH_3)_2^+ \xrightarrow{-H^+} (CH_3)_2C{=}C(CH_3)_2 \quad (8)$$

$$(CH_3)_2C{=}C(CH_3)_2 \xrightarrow[\gamma]{-e} (CH_3)_2C{=}C(CH_3)_2^{\bullet+} \quad (9)$$

carbenium ions in this mechanism (or the mechanism of formation of H-addition radicals), which are implied to be free ions, can be replaced by polar complexes with variable degree of covalent bonding to lattice oxygen atoms without changing the net chemistry. The evidence for the existence of free carbenium ions versus alkoxy complexes in zeolites has been discussed by several authors.[8-11] Our results shed no new light on this unresolved issue. We require only that Bronsted acid sites interact strongly enough with substrate molecules to cause "carbenium ion-like" transformations.

When, in contrast to the majority of the results in this study, radical cations generated radiolytically at low temperature on nonacidic zeolites are stable, transformations of the same substrates on acidic zeolites (as determined by subsequent radiolysis and EPR detection of radical cations) can be unambiguously assigned to Bronsted acid-catalyzed reactions. We have encountered such examples, and the reactions can be moderated by varying the temperature at which the sample is equilibrated prior to irradiation.[72] Thus the radiolysis/variable-temperature EPR technique provides a means of analyzing, *in situ*, the products of zeolite-catalyzed reactions as a function of zeolite, activation parameters, reaction temperature, etc. This is an active area for future work and promises to be a valuable new window on catalytic processes in zeolites.

5. Conclusion

The conclusion from the present work is that nonthermalized olefin radical cations isomerize on zeolites (nonacidic and acidic). If Bronsted acid-catalyzed transformations occur on H-ZSM-5 upon adsorption of the olefin molecules at room temperature, then the reactivity of the carbenium ion-like intermediates, in most cases, parallels that of the radical cations formed radiolytically.

Although spontaneous oxidation of alkenes has been reported on activated H-ZSM-5 and H-Mordenite,[21-28] we did not observe any EPR signals without irradiation under the conditions of our experiments. This was not a specific goal of the present work. The outstanding difference between our conditions and those that result in spontaneous oxidation is calcination of the zeolite powder in air prior to evacuation and adsorption of substrate.

The question remains, is it possible to demonstrate significant radical cation involvement in zeolite catalysis? To answer this question it will be necessary to (1) delineate the conditions that give rise to carbocations and radical cations and (2) independently elucidate the reactivity of both types of intermediates in zeolites. A systematic approach using the radiolysis technique to probe processes in zeolites with a range of acidities and other properties will advance us toward this goal. EPR detection allows the elucidation of radical cation reactions as well as the observation of radicals and radical cations of Bronsted acid-catalyzed reaction products.

Many puzzles and much promise are revealed by this and previous studies of radical cations in zeolites. Much is to be learned about what gives rise to the chemical selectivity and specificity of these unique microreactors. Nuances in reactivity result from surprisingly subtle changes in host or guest properties. Contrast the persistence of $TME^{\bullet+}$ in Na-ZSM-5 and H-ZSM-5 to its lability with respect to the ion-molecule reaction in silicalite. On the other hand, $1,3\text{-}CHD^{\bullet+}$ decays via the ion-molecule reaction in all three zeolites. The chemical selectivity is strongly influenced by the relative mobility of substrate molecules (activation energy of diffusion) but equally or more by the radical cation-matrix interactions and details of neutral adsorption.

It is apparent from failures to consistently reproduce certain results that some factors have escaped our experimental control. Thus, the relative yields of $TME^{\bullet+}$ and a second radical cation in 3,3-DMB-1-loaded H-ZSM-5 samples varied from sample to sample. E lines were observed in some, but not other, presumed identical samples. The explanation must lie partly in the details of zeolite activation and adsorption. A special challenge of zeolite studies is possible complication due to a distribution of adsorption sites that can result in sample heterogeneities. The relative population of different sites can depend on the concentration of substrate, the adsorption temperature, and the time allowed for equilibration.

It is very important that ongoing research on the chemistry of reactive intermediates in zeolites be integrated with the development of a precise physical understanding of the location and mobility of sorbate molecules and the interactions between the matrix and the neutral and charged molecules or intermediates. That means integration of EPR studies and theory, X-ray and neutron diffraction, IR absorption, isothermal adsorption, variable-temperature NMR, etc. Our present level of understanding of zeolites exceeds that of fascinating black-box reactors but falls well short of the ultimate goal that will enable us to use zeolites as versatile reactors to achieve unprecedented control of chemical reactions.

Acknowledgment. We acknowledge J. Gregar for supplying the quartz EPR cells and other glass-blowing assistance and Al Svirmickas for carrying out the ^{60}Co irradiations. We thank Dr. A. Pfenninger of Chemie Uetikon (Switzerland) for the gift of the ZSM-5 samples and the Union Carbide Co. for the gift of the silicalite-115.

References and Notes

(1) Kerr, G. T. *Sci. Am.* **1989**, 101.
(2) Breck, D. W. *Zeolite Molecular Sieves*; Wiley: New York, 1974.
(3) Ramamurthy, V. In *Photochemistry in Organized and Constrained Media*; Ramamurthy, V., Ed.; VCH: New York, 1991; p 429.

(4) *Zeolite Synthesis*; Occelli, M. L., Robson, H. E., Eds.; American Chemical Society: Washington, DC, 1989. Davis, M. E. *Acc. Chem. Res.* **1993**, *26*, 111.
(5) *Zeolite Chemistry and Catalysis*; Jacobs, P. A., et al., Eds.; Elsevier: New York, 1991.
(6) Newsam, J. M. *Science* **1986**, *231*, 1093.
(7) Corma, A. *Catal. Lett.* **1993**, *22*, 33.
(8) Rabo, J. A.; Gajda, G. *J. Catal. Rev. Sci. Eng.* **1989**, *31*, 385. Kazansky, V. B. *Acc. Chem. Res.* **1991**, *24*, 379.
(9) Gates, B. C.; Katzer, J. R.; Schuit, G. C. A. *Chemistry of Catalytic Processes*; McGraw-Hill: New York, 1979; p 1.
(10) Kramer, G. M.; McVicker, G. B.; Ziemiak, J. J. *J. Catal.* **1985**, *92*, 355.
(11) Lazo, N. D.; Richardson, B. R.; Schettler, P. D.; White, J. L.; Munson, E. J.; Haw, J. F. *J. Phys. Chem.* **1991**, *95*, 9420.
(12) Ferino, I.; Monaci, R.; Solinas, V.; Forni, L.; Rivoldini, A.; Sanseverino, L. *Collect. Czech. Chem. Commun.* **1992**, *57*, 869.
(13) Hoser, H.; Krzyzanowski, S. *J. Catal.* **1975**, *38*, 366.
(14) Kemball, C.; Leach, H. F.; Moller, B. W. *J. Chem. Soc., Faraday Trans. I* **1973**, *69*, 624.
(15) Jacobs, P. A.; Declerck, L. J.; Vandamme, L. J.; Uytterhoeven, J. B. *J. Chem. Soc., Faraday Trans. I* **1975**, *71*, 1545.
(16) Galuszka, J.; Baranski, A.; Ceckiewicz, S. *J. Chem. Soc., Faraday Trans. I* **1978**, *74*, 146.
(17) Datka, J. *J. Chem. Soc., Faraday Trans. I* **1980**, *76*, 2437.
(18) Ceckiewicz, S.; Baranski, A.; Galuszka, J. *J. Chem. Soc., Faraday Trans. I* **1978**, *74*, 2027.
(19) Langner, B. E. *J. Catal.* **1980**, *65*, 416.
(20) Karge, H. G. In *Catalysis and Adsorption by Zeolites*; Ohlmenn, G., et al., Eds.; Elsevier Science Publishers: Amsterdam, 1991; p 133.
(21) Roduner, E.; Wu, L.-M.; Crockett, R.; Rhodes, C. J. *Catal. Lett.* **1992**, *14*, 373.
(22) Roduner, E.; Crockett, R.; Wu, L.-M. *J. Chem. Soc., Faraday Trans.* **1993**, *89*, 2101.
(23) Rhodes, C. J. *J. Chem. Soc., Faraday Trans.* **1991**, *87*, 3179.
(24) Rhodes, C. J.; Standing, M. *J. Chem. Soc., Perkin Trans. 2* **1992**, 1455.
(25) Corio, P. L.; Shih, S. *J. Phys. Chem.* **1971**, *75*, 3475.
(26) Chen, F.; Guo, X. *J. Chem. Soc., Chem. Commun.* **1989**, 1682.
(27) Chen, F. R.; Fripiat, J. J. *J. Phys. Chem.* **1993**, *97*, 5796.
(28) Kucherov, A. V.; Slinkin, A. A.; Kondratyev, D. A.; Bondarenko, T. N.; Rubinstein, A. M.; Minachev, Kh. M. *J. Mol. Catal.* **1986**, *37*, 107.
(29) Qin, X.-Z.; Trifunac, A. D. *J. Phys. Chem.* **1990**, *94*, 4751.
(30) Barnabas, M. V.; Trifunac, A. D. *Chem. Phys. Lett.* **1991**, *187*, 565.
(31) Barnabas, M. V.; Trifunac, A. D. *Chem. Phys. Lett.* **1992**, *193*, 298.
(32) Barnabas, M. V.; Werst, D. W.; Trifunac, A. D. *Chem. Phys. Lett.* **1993**, *204*, 435.
(33) Barnabas, M. V.; Werst, D. W.; Trifunac, A. D. *Chem. Phys. Lett.* **1993**, *206*, 21.
(34) Cromack, K. R.; Werst, D. W.; Barnabas, M. V.; Trifunac, A. D. *Chem. Phys. Lett.* **1994**, *218*, 485.
(35) See also: Erickson, R.; Lindgren, M.; Lund, A.; Sjoqvist, L. *Colloids Surf. A* **1993**, *72*, 207. Toriyama, K.; Nunome, K.; Iwasaki, M. *J. Am. Chem. Soc.* **1987**, *109*, 4496.
(36) Lias, S. G.; Bartmess, J. E.; Liebman, J. F.; Holmes, J. L.; Levin, R. D.; Mallard, W. G. *J. Phys. Chem. Ref. Data* **1988**, *17*, (Suppl. 1).
(37) Shida, T.; Egawa, Y.; Kubodera, H.; Kato, T. *J. Chem. Phys.* **1980**, *73*, 5963.
(38) Desrosiers, M. F.; Trifunac, A. D. *Chem. Phys. Lett.* **1985**, *118*, 441.
(39) Fessenden, R. W.; Schuler, R. H. *J. Chem. Phys.* **1963**, *39*, 2147.
(40) Toriyama, K.; Nunome, K.; Iwaski, M. *Chem. Phys. Lett.* **1984**, *107*, 86. Shiotani, M.; Nagata, Y.; Sohma, J. *J. Phys. Chem.* **1984**, *88*, 4078.
(41) Qin, X.-Z.; Trifunac, A. D. Unpublished results.
(42) Williams, F.; Qin, X.-Z. *Radiat. Phys. Chem.* **1988**, *32*, 299.
(43) Desrosiers, M. F.; Trifunac, A. D. *J. Phys. Chem.* **1986**, *90*, 1560.
(44) de Tannoux, N. M.; Pratt, D. W. *J. Chem. Soc., Chem. Commun.* **1978**, 394.
(45) Griller, D.; Ingold, K. U. *J. Am. Chem. Soc.* **1974**, *96*, 6203.
(46) Iwasaki, M.; Nunome, K.; Muto, H.; Toriyama, K. *J. Chem. Phys.* **1971**, *54*, 1839.
(47) Iwasaki, M.; Toriyama, K.; Nunome, K.; Fukaya, M.; Muto, H. *J. Phys. Chem.* **1977**, *81*, 1410.
(48) Iwasaki, M.; Muto, H.; Toriyama, K.; Fukaya, M.; Nunome, K. *J. Phys. Chem.* **1979**, *83*, 1590.
(49) Wells, J. W.; Box, H. C. *J. Chem. Phys.* **1968**, *48*, 2542.
(50) Clough, S.; Poldy, F. *J. Chem. Phys.* **1969**, *51*, 2076.
(51) Davidson, R. B.; Miyagawa, I. *J. Chem. Phys.* **1970**, *52*, 1727.
(52) Freed, J. *J. Chem. Phys.* **1965**, *43*, 1710.
(53) Saitake, Y.; Miyazaki, T.; Kuri, Z. *J. Phys. Chem.* **1973**, *77*, 2418. Miyazaki, T.; Tsuruta, H.; Fujitani, Y.; Fueki, K. *J. Phys. Chem.* **1982**, *86*, 970. Miyazaki, T. *Radiat. Phys. Chem.* **1991**, *37*, 11.
(54) Werst, D. W.; Trifunac, A. D. *J. Phys. Chem.* **1988**, *92*, 1093.
(55) Nunome, K.; Toriyama, K.; Iwasaki, M. *J. Chem. Phys.* **1983**, *79*, 2499.
(56) Fujisawa, J.; Sato, S.; Shimokoshi, K.; Shida, T. *J. Chem. Phys.* **1985**, *89*, 5481.
(57) Bally, T. In *Radical Ionic Systems*; Lund, A., Shiotani, M., Eds.; Kluwer: The Netherlands, 1991; p 3.
(58) Preliminary results imply that acetylene is ionized by the irradiated zeolite. See: Cromack, K. R.; Piocos, E. A.; Werst, D. W.; Trifunac, A. D. Unpublished results.
(59) Werst, D. W.; Bakker, M. G.; Trifunac, A. D. *J. Am. Chem. Soc.* **1990**, *112*, 40.
(60) Werst, D. W.; Trifunac, A. D. *J. Phys. Chem.* **1991**, *95*, 1268.
(61) Trifunac, A. D.; Werst, D. W. In *Radical Ionic Systems*; Lund, A., Shiotani, M., Eds.; Kluwer: The Netherlands, 1991; p 195.
(62) Lund, A.; Lindgren, M.; Lunell, S.; Maruani, J. In *Molecules in Physics, Chemistry and Biology*; Maruani, J., Ed.; Kluwer: The Netherlands, 1989; Vol. 3, p 259.
(63) Toriyama, K. In *Radical Ionic Systems*; Lund, A., Shiotani, M., Eds.; Kluwer: The Netherlands, 1991; p 99.
(64) Werst, D. W.; Piocos, E. A.; Tartakovsky, E. E.; Trifunac, A. D. Work to be published.
(65) Nakazato, C.; Masuda, T. *Bull. Chem. Soc. Jpn.* **1986**, *59*, 2237. Nakazato, C.; Murayama, R.; Masayoshi, A.; Masuda, T. *Bull. Chem. Soc. Jpn.* **1986**, *60*, 2775. Aoki, M.; Nakazato, C.; Masuda, T. *Bull. Chem. Soc. Jpn.* **1987**, *61*, 1899.
(66) Wilt, J. W. In *Free Radicals*; Kochi, J. K., Ed.; Wiley: New York, 1973; Vol. 1, p 333.
(67) Kaplan, L. In *Reactive Intermediates*; Jones, M., Jr., Moss, R. A., Eds.; Wiley: New York, 1978; Vol. 1, p 163.
(68) Bartels, D. M.; Werst, D. W.; Trifunac, A. D. *Chem. Phys. Lett.* **1987**, *142*, 191.
(69) Tsai, T. E.; Griscom, D. L.; Friebele, E. J. *Phys. Rev. B* **1989**, *40*, 6374.
(70) Miyazaki, T.; Azuma, N.; Fueki, K. *J. Am. Ceram. Soc.* **1984**, *67*, 99.
(71) Bartels, D. M.; Han, P.; Percival, P. W. *Chem. Phys. Lett.* **1993**, *210*, 129.
(72) Werst, D. W.; Tartakovsky, E. E.; Piocos, E. A.; Trifunac, A. D. Unpublished results.